Available online at www.sciencedirect.com
SCIENCE DIRECT®
Journal of Power Sources 134 (2004) 110–117
JOURNAL OF POWER SOURCES
www.elsevier.com/locate/jpowsour

# $LiMn_2O_4$ prepared by different methods at identical thermal treatment conditions: structural, morphological and electrochemical characteristics

H. Gadjov [a,*], M. Gorova [a], V. Kotzeva [a], G. Avdeev [a], S. Uzunova [b], D. Kovacheva [a]

[a] *Institute of General and Inorganic Chemistry, Bulgarian Academy of Sciences, 1113 Sofia, Bulgaria*
[b] *Central Laboratory of Electrochemical Power Sources, Bulgarian Academy of Sciences, 1113 Sofia, Bulgaria*

Available online 25 May 2004

**Abstract**

Nano-crystalline $LiMn_2O_4$ materials were obtained by three different methods: thermal decomposition of mixtures of corresponding metal carbonates or nitrates, Pechini method and self-combustion reaction (SCR) method using common sugar—sucrose as a fuel. Phase composition, morphology, crystallite- and particle sizes of materials were studied by powder X-ray diffraction (XRD) and scanning electron microscopy (SEM). Contrary to thermal decomposition of metal carbonates or nitrates mixtures, Pechini and SCR methods allowed synthesis of a single-phase product at 400 °C, but the optimal temperature range for preparing of $LiMn_2O_4$ spinel with good electrochemical properties was found to be 600–650 °C. Both latter methods provided good control of the chemical composition and microstructure of the active material. The SCR method yields a fine $LiMn_2O_4$ spinel, having high initial specific capacity of 116 mA h/g and low capacity fade during cycling. The simple procedure of self-combustion method is time and energy saving, and thus is promising for commercial application.


*Keywords:* Lithium ion batteries; $LiMn_2O_4$; Self-combustion reaction method; Pechini method

## 1. Introduction

Lithium manganese oxide spinel $LiMn_2O_4$ is an interesting and promising cathode material for rechargeable lithium batteries [1–3]. In comparison with layered $LiCoO_2$ and $LiNiO_2$, its three-dimensional structure permits a reversible electrochemical extraction of the $Li^+$ ions, at about 4 V versus $Li/Li^+$, to λ-$MnO_2$ without lattice collapse [4]. Additional advantages are the relatively high theoretical capacity (148 mA h/g), low cost with ease preparation and environmental harmlessness [5]. A problem to overcome for commercial application of this material is its fast capacity fading with charge/discharge cycling [6]. This fact has been related to instability of the active phase caused by several possible factors like a slow dissolution of the cathode material into the electrolyte, high value of the relative volume changes accompanying charge/discharge cycling, Jahn–Teller distortion effect in deeply discharged electrodes [7,8]. The stoichiometry, crystal structure and morphology of the active material are of essential importance for its electrochemical properties. All these factors are closely related to the method of synthesis.

Many procedures for preparation of spinel $LiMn_2O_4$ materials have been proposed in the literature during last years. The classical ceramic synthesis by a solid-state reaction between oxides [9,10] has been used extensively, but it requires prolonged heat treatment at relatively high temperatures (>700 °C) with repeatedly intermediate grinding. Moreover, this method does not provide good control on the crystalline growth, compositional homogeneity, morphology and microstructure. As a consequence, final products consist in relatively large particles (>1 μm) with broad particle size distribution. In order to overcome these disadvantages, various preparative techniques, known as well as "soft-chemistry" methods, have been developed. Such techniques are based on the processes of co-precipitation, ion-exchange or thermal decomposition at low temperature of appropriate organic precursors obtained by sol–gel [11,12], xero-gel [13], Pechini [14,15], freeze-drying [16], emulsion-drying [17] methods. They lead to homogeneous spinel materials with small particle size but require expensive initial or intermediate reagents and involve complex preparative procedures.

* Corresponding author.
*E-mail address:* didka@svr.igic.bas.bg (H. Gadjov).

0378-7753/$ – see front matter © 2004 Elsevier B.V. All rights reserved.
doi:10.1016/j.jpowsour.2004.03.027

Very suitable to the synthesis of nano-sized oxide materials is the method of self-combustion reaction (SCR method) of metal nitrates (oxidizers) and some organic reductors (tetraformal triazine (TFTA), glycine, urea, citric acid, etc.) acting as a fuel [18–20]. The key feature of self-combustion process is that the heat needed for the synthesis of an oxide material is provided by the exothermic reaction between the fuel and the oxidizers, which are at the same time starting reagents for this product. In our previous work [21] we described the SCR synthesis of nano-sized $LiMn_2O_4$ with good electrochemical performances. The very common and cheep organic reagent—sucrose ($C_{12}H_{22}O_{11}$) has been selected as a fuel.

The aim of the present work is to find optimal conditions for thermal treatment that allow SCR synthesis of $LiMn_2O_4$ based materials with good electrochemical performance. We are of the opinion that this could be done directly by comparison of the micro-structural and electrochemical characteristics of the same compound, obtained at identical thermal conditions, by different methods like thermal decomposition of metal carbonates and nitrates or other low-temperature technique like Pechini method.

## 2. Experimental

### 2.1. Synthesis

The samples obtained were denoted as follows—sample A: thermal decomposition of carbonates, sample B: thermal decomposition of nitrates, sample C: Pechini method and sample D: SCR method.

For the synthesis of sample A, the stoichiometric amounts of $Li_2CO_3$ and $MnCO_3$ were homogenized for 30 min in an agate mortar. The powder mixture was then heated at 400 °C for 1 h.

Sample B was obtained by dissolving stoichiometric amounts of $LiNO_3$ and $Mn(NO_3)_2{\cdot}4H_2O$ in a distilled water. The solution was heated at 80 °C till evaporation of the liquid. The dry precursor was heated at 400 °C for 1 h.

Sample C was synthesized by Pechini method following the procedure given by Liu et al. [14]. The appropriate amounts of $Li_2CO_3$ and a water solution of $Mn(NO_3)_2$ were added to the solution of citric acid in ethylene glycol (1:4 molar ratio). Heating at 90 °C and vigorous stirring were applied till a clear solution was obtained. The solution was placed in a vacuum drier at 140 °C and kept there 2 h, after that the temperature was raised to 180 °C until full transformation of the solution into a resin-like substance. The as-obtained precursor was heated at 400 °C for 1 h. Resulting material was a black voluminous porous mass.

Sample D was prepared by slow evaporation and ignition of a reaction mixture containing stoichiometric amounts of Li(I) nitrate, Mn(II) nitrate and sucrose ($C_{12}H_{22}O_{11}$). The molar ratio of metal nitrates to that of the sucrose was calculated on the basis of the total oxidizing power of the nitrates and the total reducing power of the sucrose [22]. The dish containing the reaction mixture was placed on an electric heater kept at 120 °C. At this temperature the liquid started to evaporate, and the residual viscous mass of reagents transformed into brownish-yellow foam. When ignited, it burned without flame yielding a voluminous black sponge-like substance, which was then heated at 400 °C for 1 h.

The as-prepared samples A–D were divided into five equal portions. First portions were used for further XRD, SEM and electrochemical characterization. Each of the other portions was thermally treated for 2 h in air at 500, 600, 700 or 800 °C. Thermal treatment at temperature higher than 800 °C have not been carried out, since it induces oxygen and lithium vacancies in the spinel structure [23].

### 2.2. XRD and SEM characterization

Phase composition, morphology and particle sizes of the samples were studied by X-ray powder diffraction analysis (XRD) and scanning electron microscopy. XRD spectra were recorded at room temperature with computer-controlled DRON-3 powder diffractometer with Cu Kα radiation and a scintillation registration. Data were collected in the $2\theta$ range from 15° to 90° with a step 0.02° and counting time of 1 s/step. Lattice parameters were refined using the program CelRef [24]. Mean coherent domain sizes were determined by peak profile analysis with the program PowderCell [25]. Scanning electron microscopy was performed on a Phillips 515 SEM.

### 2.3. Electrochemical characterization

The effect of heating temperature and synthesis method on the electrochemical properties of $LiMn_2O_4$ samples was investigated in a three-electrode cell on a computer-controlled laboratory cycling equipment. The negative electrode was a lithium foil. The electrolyte used was a 1 M solution of $LiClO_4$ in ethylene carbonate and dimethyl carbonate (EC:DMC = 1:1 ratio). The water content of the electrolyte was less than 30 ppm. Positive electrode composites were prepared from spinel $LiMn_2O_4$ powder (15 mg) with teflonized acetylene black (TAB) (1:1 weight ratio). The obtained mass was pressed onto an aluminum foil (15 mm diameter). All cell assemblies were carried out in argon filled dry box. The cells were cycled at room temperature in the voltage range 3.0–4.2 and 3.0–4.5 V versus $Li/Li^+$. The current density was $C/3$ (0.42 mA/cm$^2$), where $C$ is the capacity of the electrode calculated on the basis of the theoretical capacity of $LiMn_2O_4$ (148 mA h/g).

## 3. Results and discussion

### 3.1. Phase composition and microstructure

XRD powder patterns of the samples obtained by thermal decomposition of carbonates (A) and nitrates (B) at

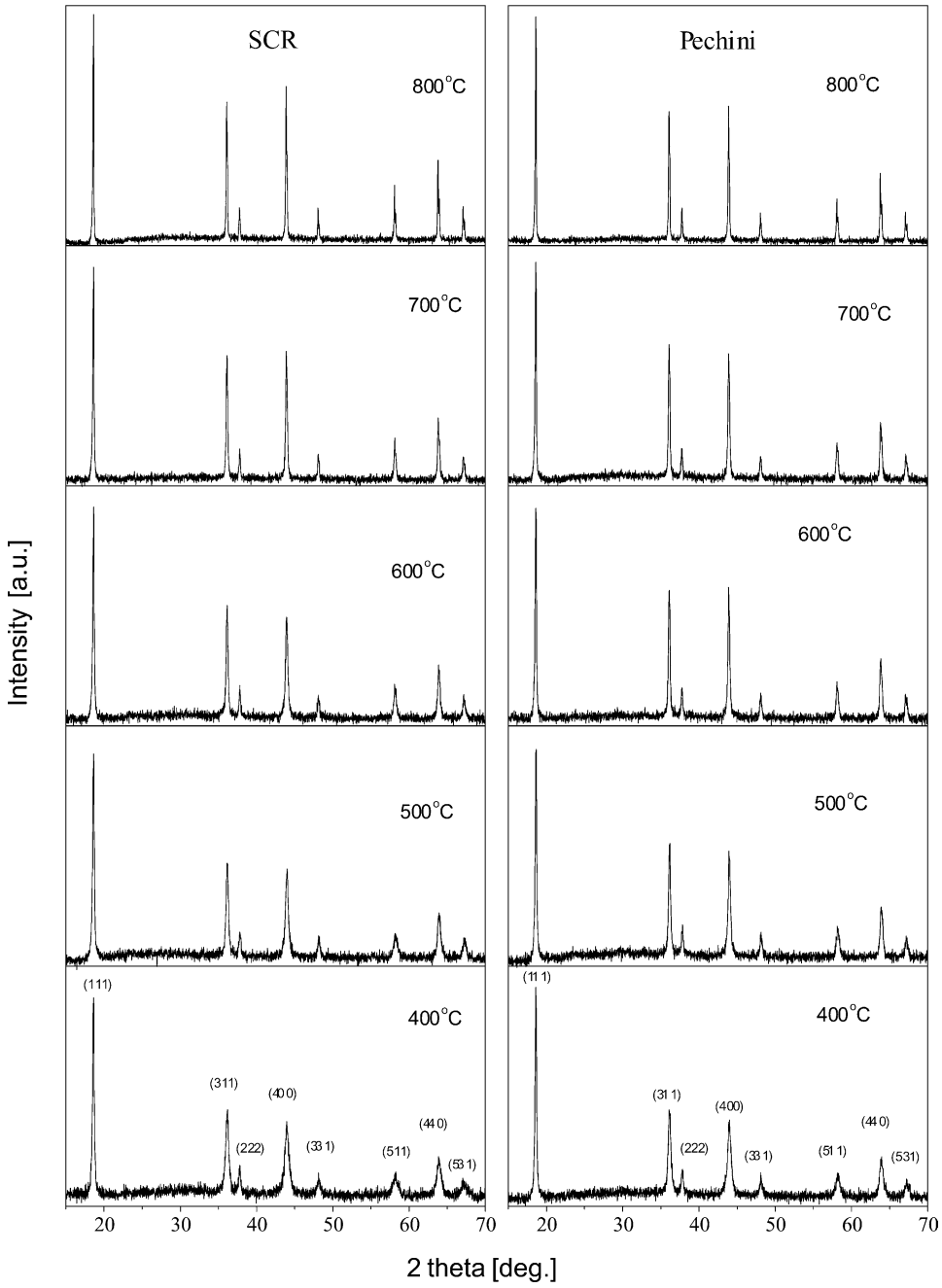


Fig. 1. XRD spectra of samples C (right column) and D (left column) heated at different temperatures.

temperatures below 800 °C contain peaks of spinel phase along with peaks of some intermediate manganese oxide phases. XRD pattern of sample A heated at 400 °C shows poorly crystallized $Mn_2O_3$ and a spinel phase. Upon further thermal treatment at 500–700 °C the quantity of the $Mn_2O_3$ phase decreases and its XRD peaks disappeared after heating at 800 °C. XRD pattern of sample B fired at 400 °C shows peaks of a spinel phase and peaks of β-$MnO_2$. At 500 °C $MnO_2$ transforms to $Mn_2O_3$, the latter being present in samples heated up to 700 °C. Synthesis of single-phase product by both methods requires heating at 800 °C, at least. At such elevated temperatures, phase homogeneity is achieved by long-range cation diffusion transport but, at the same time, the particle size increases rapidly beyond the optimum limits.

Powder XRD patterns of the spinel $LiMn_2O_4$ prepared by Pechini (C) and SCR (D) methods and heated at different temperatures are shown in Fig. 1. It is seen that single-phase products were obtained by both methods at 400 °C. Further heating at higher temperature leads to gradual sharpening of the diffraction peaks which is an indication of the improved crystallinity of the samples. This fact was confirmed by

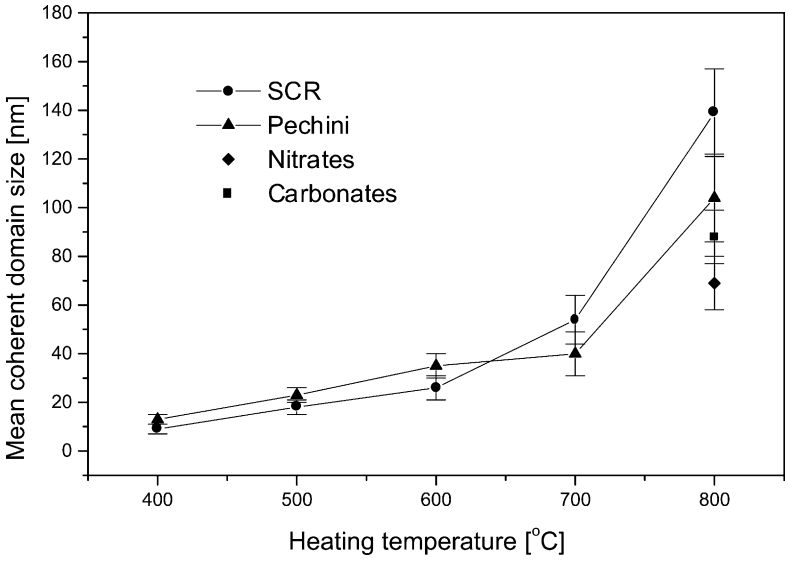


Fig. 2. Dependence of the mean coherent domain size on heating temperatures.

detailed analysis of the peak broadening combined with scanning electron microscopy. The mean coherent domain size (MCDS), calculated by line profile analysis, for samples C and D increases from 10–15 nm at 400 °C to 100–140 nm at 800 °C (Fig. 2). The relatively lower (70–90 nm) MCDS of the spinel phase in samples A and B heated 2 h at 800 °C shows that a reaction between intermediate oxides and the formation of spinel product took place, but this heating

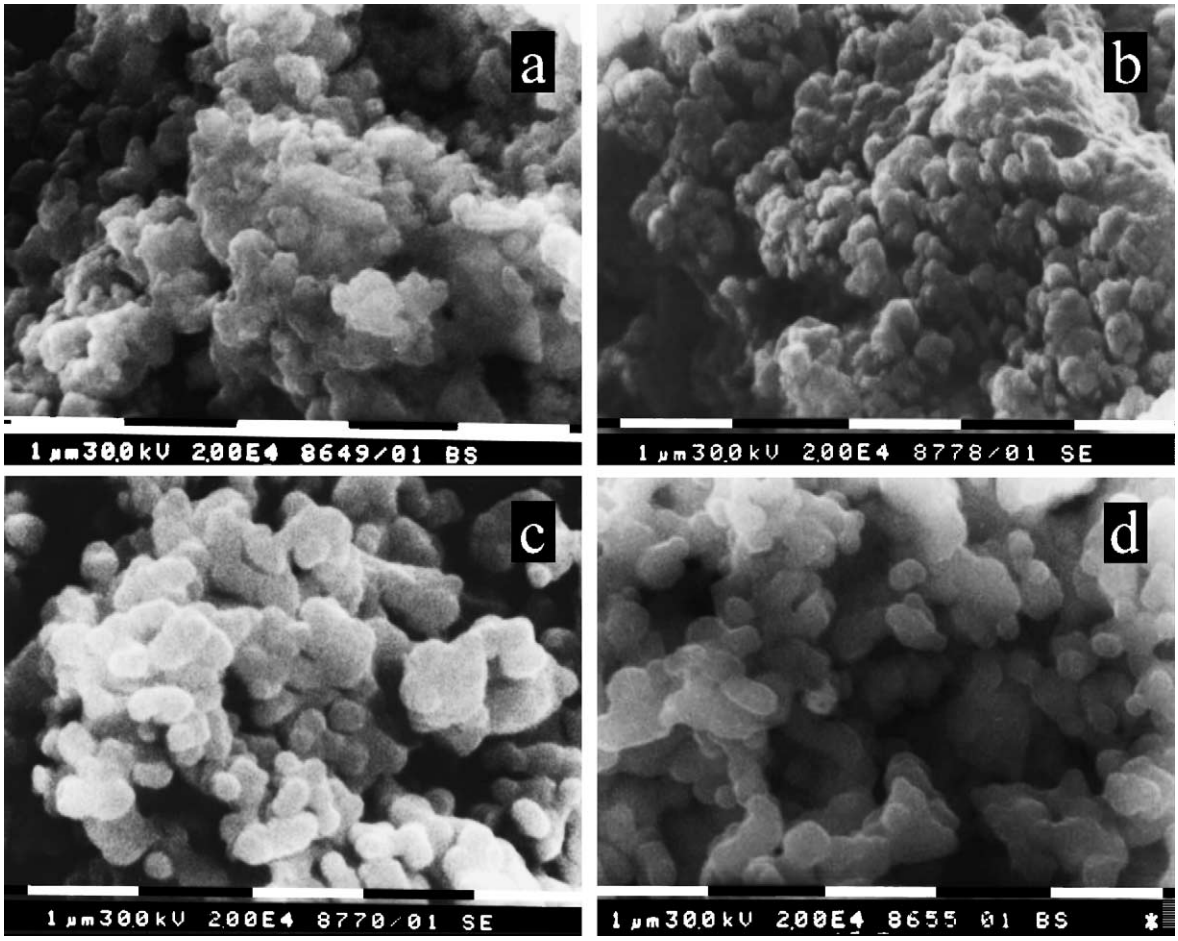


Fig. 3. SEM photographs of samples C (right) and D (left) heated at 500 °C ((a) and (b)) and 800 °C ((c) and (d)).

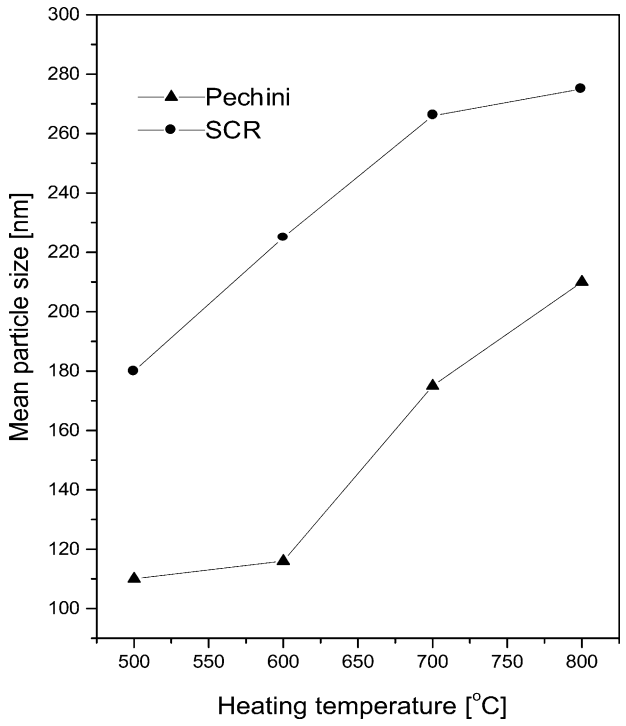


Fig. 4. Dependence of the mean particle size on heating temperature.

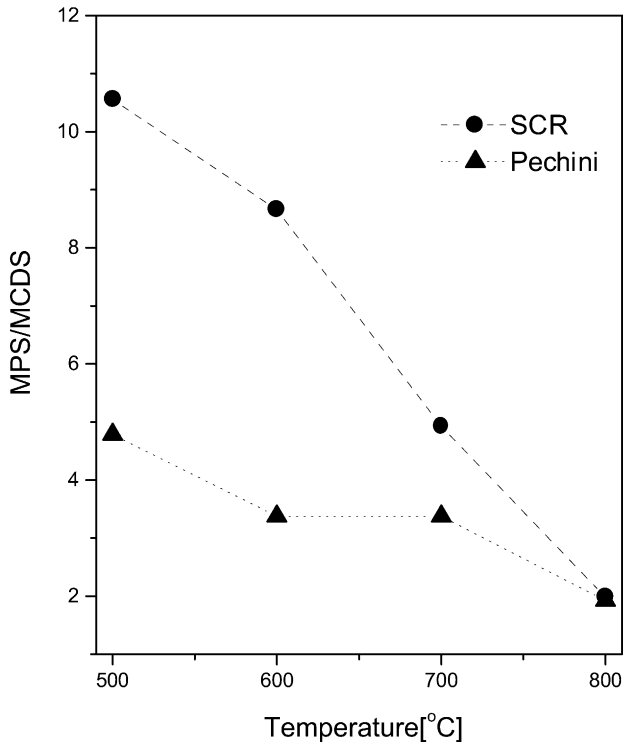


Fig. 5. Evolution of the ratio of the mean particle size (nm)/mean coherent domain size (nm) with heating temperature.

time was not sufficient for the formation of a stoichiometric well-crystallized material.

SEM photographs of samples C and D, heated at 500 and 800 °C, are presented in Fig. 3. For both samples treated at 500 °C aggregates of relatively small globular particles with uniform size of about 90–100 nm are seen. The mean particle size (MPS) increases with heating temperature, reaching value of about 200–300 nm at 800 °C, as can be seen from Fig. 4.

It is well known that cathode material with good electrochemical performance should have high chemical diffusion coefficient of lithium [26]. Lithium diffusion depends not only on the compositional homogeneity, size and morphology of the material, but also on the porosity and microstructure, resulting from the presence of different type of defects like point defects, dislocations, twin boundaries, grain boundaries. The difference between the microstructure of the products obtained by Pechini and SCR methods is seen in Fig. 5, where the evolution of the ratio mean particle size (nm)/mean coherent domain size (nm) with heating temperature is presented. This ratio is a measure of the number of the coherent scattering domains within one particle, and also the measure of defect structure since coherent scattering domains are separated by the defects presented in the material. Observed difference may be regarded as a consequence of the different defect structure of the materials prepared by the two methods. At low temperature the SCR method leads to the formation of highly defect materials, due to the large amount of gases evolved during the combustion reaction. At the same temperature the Pechini method produces material with lower amount of defects. At high temperature the materials obtained by both methods show similar micro-structural characteristics.

The dependence of the unit cell parameters on the heating temperature, for the samples synthesized by the above described methods, is shown in Fig. 6. The lattice parameters of samples A and B remain lower than the standard 8.248 Å of the stoichiometric $LiMn_2O_4$ [27], even at 800 °C, revealing that 2 h thermal treatment is not enough for obtaining stoichiometric material.

At 400 and 500 °C the lattice parameters for samples C and D are close, but remain somewhat lower. After heating at temperatures higher than 600 °C they gradually increase to the standard value. This behavior advocates that product materials have Li/Mn ratio very close to the stoichiometric one, 1:2, but the phase synthesized at low temperature is over-oxidized cation-deficient spinel. This fact is not surprising, because it is well known that non-homogeneous and defect products are usually obtained at the low-temperature stages of the synthesis procedures, based on decomposition of organic precursors [28].

### 3.2. Electrochemical behavior

The initial discharge capacities in a potential range from 3.0 to 4.2 V of sample D heated at different temperatures, are shown in Fig. 7. All discharge curves exhibit two plateaus at about 4.0–4.1 and 3.9–4.0 V. The appearance of such plateaus in the charge/discharge curves is associated

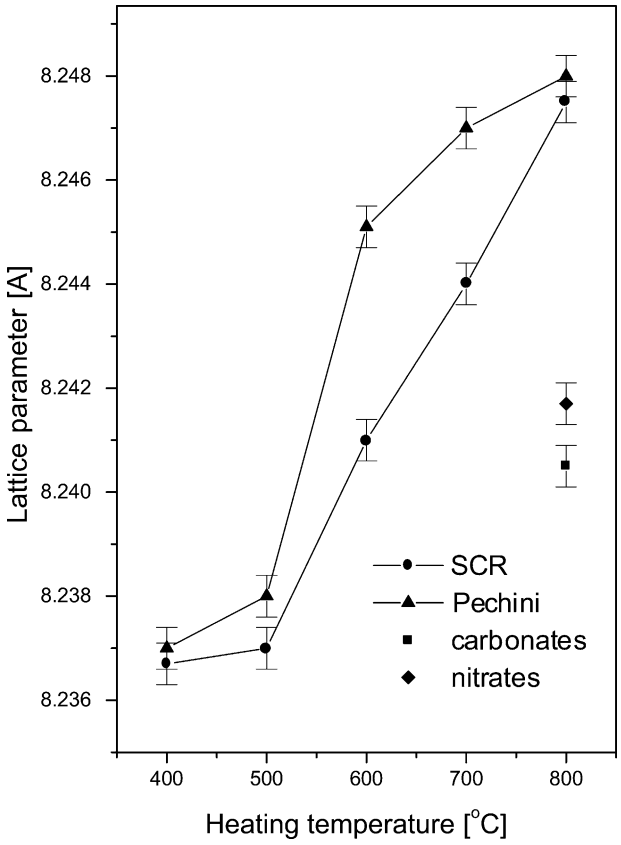


Fig. 6. Dependence of the lattice parameters on heating temperature.

with two-stage mechanism of the electrochemical lithium intercalation [29]. These plateaus become more pronounced with increasing the heating temperature which is usually attributed to the improvement of the crystallinity and diminution of the number of structure defects of the samples [11]. The initial discharge capacity for samples A and B heated at 800 °C for 2 h are 93 and 95 mA h/g, respectively. The initial discharge capacity of sample C depends on the heating temperature but is lower than this observed for sample D, as can be seen in Fig. 8, where the dependence of the specific discharge capacity on the firing temperature for samples C and D is presented. It also can be seen that for both samples the discharge capacity increases with heating temperature up to 600 °C and slightly decreases above this temperature. The increase of the lattice parameters at temperatures higher than 600 °C reveals the improved stoichiometry of the samples, and leads to the expectation of improvement of their electrochemical performances. However, it was not observed for samples C and D, implying that there are other factors in the thermal treatment process that affect electrochemical behavior in a negative way. Among them, it may be mentioned the oxygen loss at temperature above 800 °C, the diminution of the microstructure defects and increase of particle size. In the present experiment the influence of the first factor was reduced, since the maximum heating temperature was chosen to be 800 °C. We suggest that observed slight decrease of the discharge capacity comes from the other two factors which govern the micro-structural characteristics of both samples with thermal treatment. Improvement of homogeneity and crystallinity of materials takes place between 400 and 600 °C. At higher temperatures an undesirable fast increase of particle size is observed. On the other hand, spinels obtained at 400–500 °C are over-oxidized having excess amount of $Mn^{4+}$ and higher temperature is needed to reduce its quantity to the stoichiometric one. Obviously, for Pechini and SCR methods, in the temperature's range 600–650 °C occurs balance between the above mentioned

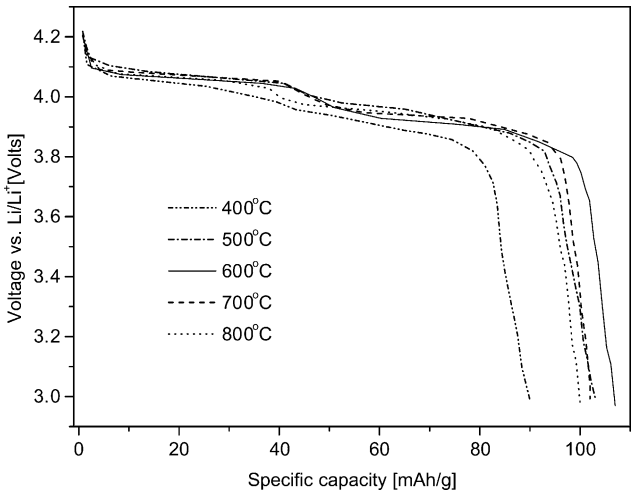


Fig. 7. Initial specific discharge capacities in a potential range 3.0–4.2 V of sample D heated at different temperatures.

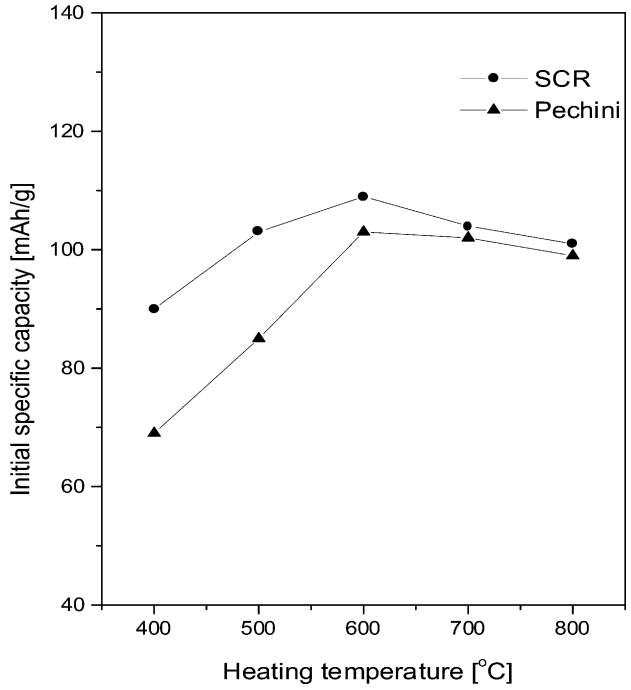


Fig. 8. Dependence of the initial discharge capacities for samples C and D on heating temperature.

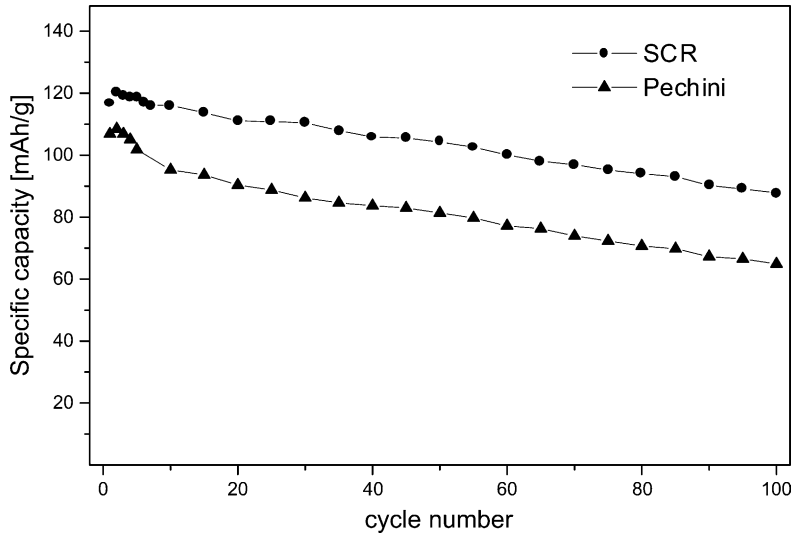


Fig. 9. Variation of the discharge capacity as a function of cycle number for samples C and D heated at 600 °C, at a *C*/3 rate in a potential range 3.0–4.5 V.

Table 1
Calculated fading rate at different stages of the cycling process for samples C and D according to the equations: $(Q_n - Q_m)/N$ (mA h/g cycle) and $[(Q_n - Q_m)/Q_n N] \times 100\%$, where $Q_n$, $Q_m$ are the discharge capacities observed at the *n*th and *m*th cycle and *N* is the number of cycles

| Cycles | Fading rate per cycle | |
|---|---|---|
| | Sample C (Pechini) | Sample D (SCR) |
| 1–30 | 0.59 mA h/g (0.55%) | 0.18 mA h/g (0.15%) |
| 30–100 | 0.32 mA h/g (0.36%) | 0.32 mA h/g (0.29%) |
| 1–100 | 0.40 mA h/g (0.37%) | 0.28 mA h/g (0.24%) |

contradictory factors resulting in the synthesis of $LiMn_2O_4$ spinel with good initial specific capacity.

The initial discharge capacity is not unique electrochemical characteristic. For more reasons the cycling stability of the cathode material is also very important. The specific discharge capacity in a potential range 3.0–4.5 V versus cycle number for samples C and D is presented in Fig. 9. Calculated fading rates for both samples at different stages of the cycling are presented in Table 1. Material prepared by Pechini method shows initial decline of capacity during the first 30 cycles, while spinel prepared by SCR method shows small fading rate at the same cycling stage. Moreover, sample D retains lower fading rate than sample C up to the 100th cycle. Better initial discharge capacity for sample D is accompanied with better cycling stability.

## 4. Conclusions

$LiMn_2O_4$ spinel cathode materials were prepared by different methods in order to compare their characteristics. Low-temperature techniques (Pechini and SCR methods) allow synthesis of a single-phase product at 400 °C. They provide better control of the composition, morphology and electrochemical properties of the active material, making them preferable to the classical solid-state reaction methods. The optimal temperature for the synthesis of $LiMn_2O_4$ spinel with good initial specific capacity by both methods was found to be 600–650 °C.

The SCR method yields a fine $LiMn_2O_4$ spinel, which is suitable for preparation of nano-crystalline cathode materials with high initial discharge capacity and very good cycling behavior. The simple procedure of the combustion method is time and energy saving, and thus is appropriate for commercial application.

## References

[1] M.M. Thackeray, W.I.F. David, P.G. Bruce, J.B. Goodenough, Mater. Res. Bull. 18 (1983) 461.
[2] M. Tarascon, E. Wang, F.K. Shokoohi, W.R. McKinnon, S. Colson, J. Electrochem. Soc. 138 (1991) 2859.
[3] C. Julien, Z. Stoynov, Materials for Lithium-ion Batteries, NATO Sciences Series, Kluwer Academic Publishers, Dordrecht, 1999.
[4] M.M. Thackeray, P.J. Johnson, L.A. Picciotto, P.G. Bruce, J.B. Goodenough, Mater. Res. Bull. 19 (1984) 179.
[5] J. Tarascon, W. Mckinnon, F. Coowar, T. Bownmer, G. Matucci, D. Guyomard, J. Electrochem. Soc. 141 (1994) 1421.
[6] A. Momchilov, V. Manev, A. Nassalevska, J. Power Sour. 43 (1993) 305.
[7] J. Rodriguez-Carvajal, G. Rousse, C. Masquelier, M. Hervieu, Phys. Rev. Lett. 81 (1998) 4660.
[8] R.J. Gummow, A. de Kock, M.M. Thackeray, Solid State Ionics 69 (1994) 59.
[9] J. Guan, M. Liu, Solid State Ionics 110 (1998) 21.
[10] G. Li, A. Yamada, Y. Fukushima, K. Yamaura, T. Saito, T. Endo, H. Azuma, K. Sekai, Y. Nishi, Solid State Ionics 130 (2000) 221.
[11] L. Hernan, J. Morales, L. Sanchez, J. Santos, Solid State Ionics 104 (1997) 205.
[12] S. Kang, J. Goodenough, J. Electrochem. Soc. 147 (2000) 3621.
[13] S.R. Prabaharan, M.S. Michael, T.P. Kumar, A. Mani, K. Athinarayanaswami, R. Gangadharan, J. Mater. Chem. 5 (1995) 1035.

[14] W. Liu, G.C. Farrington, F. Chaput, B. Dunn, J. Electrochem. Soc. 143 (1996) 879.
[15] W. Liu, K. Kowal, G.C. Farrington, J. Electrochem. Soc. 143 (1996) 3590.
[16] E. Zhecheva, M. Gorova, R. Stoyanova, J. Mater. Chem. 9 (1999) 1559.
[17] K. Hwang, W. Um, H. Lee, J. Song, K. Chung, J. Power Sour. 74 (1998) 169.
[18] N. Arul Dhas, K. Patil, J. Solid State Chem. 102 (1993) 440.
[19] W. Yang, G. Zhang, J. Xie, L. Yang, Q. Liu, J. Power Sour. 81–82 (1999) 412.
[20] K. Lee, H. Choi, J. Lee, J. Mater. Sci. Lett. 20 (2001) 1309.
[21] D. Kovacheva, H. Gadjov, K. Petrov, S. Mandal, M.G. Lazarraga, L. Pascual, J.M. Amarilla, R.M. Rojas, P. Herrero, J.M. Rojo, J. Mater. Chem. 12 (2002) 1184.
[22] M. Sekar, K. Patil, J. Mater. Chem. 2 (1992) 739.
[23] M. Palacin, Y. Chabre, L. Dupont, M. Hervieu, P. Strobel, G. Rousse, C. Masquelier, M. Anne, G. Amatucci, J. Tarascon, J. Electrochem. Soc. 147 (2000) 845.
[24] J. Laugier, A. Filhol, CelRef, PC Version, ILL, Grenoble, France, unpublished, 1991.
[25] W. Kraus, G. Nolze, PowderCell Program for Windows, Version 2.4, BAM, Berlin, 2000.
[26] L. Chen, X. Huang, E. Kelder, J. Schoonman, Solid State Ionics 76 (1995) 91.
[27] JCPDS-ICDD, PDF No. 35-782.
[28] A. Manthiram, J. Kim, Chem. Mater. 10 (1998) 2895.
[29] W. Liu, K. Kowal, G. Farrington, J. Electrochem. Soc. 145 (1998) 459.